Energy norm error estimates and convergence analysis for a stabilized Maxwell's equations in conductive media

E. Lindström * L. Beilina †

December 21, 2023

Abstract

The aim of this article is to investigate the well-posedness, stability and convergence of solutions to the time-dependent Maxwell's equations for electric field in conductive media in continuous and discrete settings. The situation we consider would represent a physical problem where a subdomain is emerged in a homogeneous medium, characterized by constant dielectric permittivity and conductivity functions. It is well known that in these homogeneous regions the solution to the Maxwell's equations also solves the wave equation which makes calculations very efficient. In this way our problem can be considered as a coupling problem for which we derive stability and convergence analysis. A number of numerical examples validate theoretical convergence rates of the proposed stabilized explicit finite element scheme.

Keywords: *Maxwell's equations, finite element method, stability, a priori error analysis, energy error estimate, convergence analysis*
Mathematics Subject Classification (2010): 65N15, 65N21, 65N30, 35Q61

1 Introduction

In this paper we consider the time-dependent Maxwell's equations in a bounded, simply connected spatial domain Ω. This domain is divided into two subdomains, one outer were the dielectric permittivity and conductivity are constant functions, and one inner one were they are allowed to vary but are still bounded functions.

One important (and of special interest for the authors) consequence of the results developed in this paper are applications of Maxwell's equations to solutions of *Coefficient Inverse Problems* (CIPs). In [39, 40] one can read about inverse problems applied to imaging of buried objects, and in [8, 9, 13] inverse problems are used for medical

*Eric Lindström, Email: erilinds@chalmers.se
†Larisa Beilina, Email: larisa@chalmers.se
Department of Mathematical Sciences, Chalmers University of Technology and University of Gothenburg, SE-412 96 Gothenburg Sweden

imaging. In the latter case the problem is to reconstruct the dielectric permittivity and conductivity functions of an anatomically realistic phantom of a breast tissue. The dielectric properties of different tissue types in a breast are experimentally measured and known [25], but their distribution inside every particular breast tissue is unknown. Such a scenario is one case where the domain decomposition can be an useful tool for solution of electromagnetic CIPs when the goal is determination of dielectric properties of the object from boundary measurements of the scattered electric field.

Under certain circumstances, it is known that the solution to the Maxwell's equations also solves the wave equation, which is more studied and understood, see [4, 5, 7, 8, 10]. In [10], a finite element analysis shows stability and consistency of the stabilized finite element method for the solution of Maxwell's equations in non-conductive media, and in [4] authors investigated a stabilized domain decomposition finite element method for the time harmonic Maxwell's equations. Stability and convergence analysis of a Domain Decomposition FE/FD method for time-dependent Maxwell's equations was presented in [5]. In our knowledge, all previous cited works consider non-conductive media, and the research concerning time-dependent Maxwell's equation for electric field in conductive media, when both dielectric permittivity and conductivity are space-dependent functions, are missing.

The stability and well-posedness of the wave equation are well understood and studied [23, 31]. Certain model of wave equations have also been used to model inverse problems, see [11, 6, 24]. The progression to Maxwell's equations is arguably natural, since the system has wave-like properties. However, some complications occur from the presence of the double curl operator. Another theoretical complication is that when one analyzes the corresponding bilinear form induced by the variational form, one can see that it is not coercive. This coercivity is often critical in proofs concerning existence and uniqueness of solutions. The additional novelty of the presented work is in how we deal with coercivity of the bilinear form. Since the bilinear form with presence of time-dependent terms is non-coercive, we split it and separate terms with derivatives in time in order to derive the coercivity for the remaining spatial part of the bilinear form using some minor restrictions on the gradient of the permittivity function. We use then coercivity of the spatial part of the bilinear form in the proof of a priori error estimate. Derivation of coercivity of the entire scheme is a topic of an ongoing research.

To align the results with implementations of $P1$-methods, we introduce a slightly altered, stabilized problem. Otherwise, these methods can lead to spurious solutions (see [3, 7, 15, 16, 26, 27, 28, 29, 35, 37]) and is well-known that theoretically, divergence free edge edge elements are a better fit, see [17, 21, 33, 34, 36]. To read more about various numerical methods for Maxwell equations and more details about the complications, see [2, 3, 4, 14, 18, 19, 21, 22, 33, 35] and references therein. Naturally, since the theoretical results of this work have importance for numerical implementations, we also present analysis of the corresponding discrete problem to our original pmodel.

An outline of this paper is as follows. In Section 2 we introduce the mathematical model and present the stabilized problem for the time-dependent Maxwell's equations in conductive media. In Section 3 we state the variational problem for the stabilized model and formulate the finite element scheme. Section 4 is devoted to the energy norm error analysis and section 5 presents derivation of a priori error estimates. In

Section 6 are performed numerical convergence tests illustrating theoretical results of this paper. Finally, in Section 7 we conclude the results of the paper.

2 The mathematical model

Let us consider the initial value problem for the electric field $E(x,t) = (E_1, E_2, E_3)(x,t)$, $x \in \mathbb{R}^3$, $t \in [0,T]$, for time-dependent Maxwell's equations in conductive media, under the assumptions that the dimensionless relative magnetic permeability of the medium is $\mu_r \equiv 1$:

$$\begin{aligned} \frac{1}{c^2}\varepsilon_r(x)\frac{\partial^2 E}{\partial t^2} + \nabla\times\nabla\times E &= -\mu_0\sigma(x)\frac{\partial E}{\partial t} - j, \\ \nabla\cdot(\varepsilon E) &= 0, \\ E(x,0) = f_0(x), \quad \frac{\partial E}{\partial t}(x,0) &= f_1(x), \;\; x\in\mathbb{R}^3, t\in(0,T]. \end{aligned} \tag{1}$$

Here, $\varepsilon_r(x) = \varepsilon(x)/\varepsilon_0$ is the dimensionless relative dielectric permittivity, $\sigma(x)$ is the electric conductivity function; ε_0, and μ_0 are the permittivity and permeability of the free space, respectively, and $c = 1/\sqrt{\varepsilon_0\mu_0}$ is the speed of light in free space and j is a given source function.

To solve the problem (1) numerically, we consider it in a bounded simply connected space domain $\Omega \subset \mathbb{R}^n$, $n = 2,3$ with boundary Γ and time domain $J = (0,T)$. In this work we will study the problem (1) in a special framework: we decompose the space domain Ω into two subdomains such that $\Omega = \Omega_1 \cup \Omega_2, \Omega_1 \subset \Omega$ and $\Omega_1 = \Omega_{\text{IN}} \cup \Omega_{\text{OUT}}$. We assume that for some known constants $d_1 > 1, d_2 > 0$ chosen such that $d_1 > d_2$, the functions $\varepsilon, \sigma \in C^2(\Omega)$ satisfy following conditions:

$$\begin{aligned} &\varepsilon_r(x) \in [1, d_1], \quad \sigma(x) \in [0, d_2], \;\; \text{for } x \in \Omega_{\text{IN}}, \\ &\varepsilon_r(x) = 1, \quad \sigma(x) = 0 \quad \text{for } x \in \Omega_2 \cup \Omega_{\text{OUT}}. \end{aligned} \tag{2}$$

We refer to [8] and references therein for justification and possible choice of these coefficients.

We observe that conditions (2) on ε and σ together with the relation

$$\nabla\times\nabla\times E = \nabla(\nabla\cdot E) - \nabla\cdot(\nabla E), \tag{3}$$

and divergence free condition $\nabla\cdot(\varepsilon E) = 0$ in Ω_2, make equations in (1) independent of each others in Ω_2 such that in Ω_2, we solve the system of uncoupled wave equations:

$$\frac{\partial^2 E}{\partial t^2} - \Delta E = 0, \quad (x,t) \in \Omega_2 \times (0,T]. \tag{4}$$

In [10], a finite element analysis shows stability and consistency of the stabilized finite element method for the solution of (1) with $\sigma(x) = 0$. In [4] a stabilized linear, domain decomposition finite element method for the time harmonic Maxwell's equations was studied. In the current study we show stability and convergence analysis of the finite element method for solution of (1) under the condition (2) on ε and σ.

Let $\Omega_T = \Omega \times (0,T), \Gamma_T = \Gamma \times (0,T)$. Let us introduce the following spaces of real valued functions

$$
\begin{aligned}
H_E^2(\Omega_T) &:= \{w \in H^2(\Omega_T) : w(\cdot,0) = f_0, \frac{\partial w}{\partial t}(\cdot,0) = f_1\}, \\
H_E^1(\Omega_T) &:= \{w \in H^1(\Omega_T) : w(\cdot,0) = f_0, \frac{\partial w}{\partial t}(\cdot,0) = f_1\}.
\end{aligned} \tag{5}
$$

In this paper we study the following stabilized initial boundary value problem setting $\mathbf{H}_E^2(\Omega_T) = [H_E^2(\Omega_T)]^3$: find $E \in \mathbf{H}_E^2(\Omega_T)$ such that

$$
\begin{cases}
\varepsilon \frac{\partial^2 E}{\partial t^2} - \triangle E - \nabla(\nabla \cdot ((\varepsilon - 1)E)) = -\sigma(x)\frac{\partial E}{\partial t} - j & \text{in } \Omega_T, \\
E(\cdot,0) = f_0(\cdot), \text{ and } \partial_t E(\cdot,0) = f_1(\cdot) & \text{in } \Omega, \\
E = 0 & \text{on } \Gamma_T.
\end{cases} \tag{6}
$$

Here, the divergence free condition $\nabla \cdot (\varepsilon E) = 0$ is hidden in the first equation of system (6).

3 Finite Element Discretization

Throughout the paper we denote the inner product in space of $[L^2(\Omega)]^d, d \in \{1,2,3\}$, by $(\cdot,\cdot)$, and the corresponding norm by $\|\cdot\|$.

Let us define the following L_2 scalar products used in the analysis:

$$
\begin{aligned}
(u,v) &:= (u,v)_\Omega = \int_\Omega uv \, d\mathbf{x}, \quad ((u,v)) := ((u,v))_{\Omega_T} = \int_0^T \int_\Omega uv \, d\mathbf{x}dt, \\
\langle u,v \rangle &:= \langle u,v \rangle_\Gamma = \int_\Gamma uv \, d\sigma, \quad \langle\langle u,v \rangle\rangle := \langle\langle u,v \rangle\rangle_{\Gamma_T} = \int_0^T \int_\Gamma uv \, d\sigma dt.
\end{aligned} \tag{7}
$$

Additionally, we define the ω-weighted $L^2(\Omega)$ norm

$$
\|u\|_\omega := \sqrt{\int_\Omega \omega |u|^2 \, d\mathbf{x}}, \qquad \omega > 0, \quad \omega \in L^\infty(\Omega) \tag{8}
$$

together with the ω-weighted L_2 scalar product:

$$
(u,v)_\omega := \int_\Omega \omega \; uv d\mathbf{x}. \tag{9}
$$

To write finite element scheme to solve the model problem (6) in whole Ω, we discretize $\Omega_T = \Omega \times (0,T)$ by partition $K_h = \{K\}$ of Ω into elements K, where $h = h(x)$ is a mesh function defined as $h = \max_{K \in K_h} h_K$. Here, where h_K denotes the local diameter of the element K. We also denote by $\partial K_h = \{\partial K\}$ a partition of the boundary Γ into boundaries ∂K of the elements K. Let J_τ be a uniform partition of the time interval $(0,T)$ into N equidistance subintervals $J = (t_{k-1}, t_k]$ with the time step $\tau = T/N$. We also assume a minimal angle condition on elements K in K_h [1, 32].

To formulate the finite element method for the spatial semi-discrete problem (6) in Ω we introduce the finite element space $W_h^E(\Omega)$ for every component of the electric field E defined by

$$W_h^E(\Omega) := \{w \in H^1(\Omega) : w|_K \in P_1(K), \forall K \in K_h\},$$

where $P_1(K)$ denote the set of piecewise-linear functions on K. We define f_{0h}, f_{1h}, j_h to be the usual interpolants of f_0, f_1, j, respectively, in (6) onto $[W_h^E(\Omega)]^3$.

Setting $\mathbf{W}^E(\Omega) = [W^E(\Omega)]^3$ and $\mathbf{W}_h^E(\Omega) = [W_h^E(\Omega)]^3$ where the test function space is chosen as

$$\mathbf{W}_{h,0}^E(\Omega) := \{\mathbf{v} \in \mathbf{W}_h^E(\Omega) \mid \mathbf{v} = 0 \quad \text{on} \quad \Gamma\}, \tag{10}$$

the spatial semi-discrete problem (6) in Ω reads:

Find $E_h \in \mathbf{W}_h^E(\Omega)$ *such that* $\forall \mathbf{v} \in \mathbf{W}_{h,0}^E(\Omega)$,

$$\begin{aligned} B(E_h, \mathbf{v}) := (\varepsilon \partial_{tt} E_h, \mathbf{v}) + (\sigma \partial_t E_h, \mathbf{v}) + a(E_h, \mathbf{v}) &= -(j, \mathbf{v}), \\ E_h(\cdot, 0) &= f_{0h}(\cdot), \\ \partial_t E_h(\cdot, 0) &= f_{1h}(\cdot) \quad \text{in } \Omega. \end{aligned} \tag{11}$$

Here, a is a bilinear form defined as

$$\begin{aligned} a(E_h, \mathbf{v}) := &(\nabla E_h, \nabla \mathbf{v}) + (\nabla \cdot ((\varepsilon - 1)E_h), \nabla \cdot \mathbf{v}) \\ &- (n \cdot \nabla \cdot ((\varepsilon - 1)E_h), \nabla \cdot \mathbf{v})_{\partial\Omega} - \langle \partial_n E_h, \mathbf{v} \rangle_\Gamma \end{aligned} \tag{12}$$

We observe that boundary terms in (12) disappear because of definition of test space (10). Thus, the bilinear form (12) for the case of test space (10) will be transformed to

$$a(E_h, \mathbf{v}) := (\nabla E_h, \nabla \mathbf{v}) + (\nabla \cdot ((\varepsilon - 1)E_h), \nabla \cdot \mathbf{v}). \tag{13}$$

Let us recall the explicit fully discrete finite element scheme for solution of (11) for $k = 1, 2, \ldots, N-1$ and $\forall \mathbf{v} \in \mathbf{W}_{h,0}^E(\Omega)$ which was derived in [9]:

$$\begin{aligned} &\left(\varepsilon_h \frac{E_h^{k+1} - 2E_h^k + E_h^{k-1}}{\tau^2}, \mathbf{v}\right) + (\nabla E_h^k, \nabla \mathbf{v}) + (\nabla \cdot (\varepsilon_h E_h^k), \nabla \cdot \mathbf{v}) - (\nabla \cdot E_h^k, \nabla \cdot \mathbf{v}) \\ &+ (\sigma_h \frac{E_h^{k+1} - E_h^{k-1}}{2\tau}, \mathbf{v}) + (j_h^k, \mathbf{v}) = 0, \\ &{E_h}^0 = f_{0h} \text{ and } {E_h}^1 = {E_h}^0 + \tau f_{1h} \text{ in } \Omega. \end{aligned} \tag{14}$$

In the scheme (14) we approximated $E_h(k\tau)$ and $j_h(k\tau)$ by E_h^k and j_h^k, respectively, for $k = 1, 2, ..., N$. Rearranging terms in (14) we get for $k = 1, 2, \ldots, N-1$ and $\forall \mathbf{v} \in \mathbf{W}_{h,0}^E(\Omega)$

$$\begin{aligned} &\left((\varepsilon_h + \frac{\tau}{2}\sigma_h)E_h^{k+1}, \mathbf{v}\right) = \left(2\varepsilon_h E_h^k, \mathbf{v}\right) - \left(\varepsilon_h E_h^{k-1}, \mathbf{v}\right) - \tau^2(\nabla E_h^k, \nabla \mathbf{v}) \\ &- \tau^2(\nabla \cdot (\varepsilon_h E_h^k), \nabla \cdot \mathbf{v}) + \tau^2(\nabla \cdot E_h^k, \nabla \cdot \mathbf{v}) \\ &+ \tau(\frac{\sigma_h}{2} E_h^{k-1}, \mathbf{v}) - \tau^2(j_h^k, v), \\ &E_h^0 = f_{0h} \text{ and } E_h^1 = E_h^0 + \tau f_{1h} \text{ in } \mathbf{\Omega}. \end{aligned} \tag{15}$$

For the convergence of this scheme the following CFL condition derived in [10] for the case of $\sigma = 0$ should hold:

$$\tau \leq \frac{h}{\eta}, \eta = C\sqrt{1 + 3\|\varepsilon - 1\|_{\infty}}, \tag{16}$$

where C is a mesh independent constant. The CFL condition for the case when both functions $\varepsilon \neq 0, \sigma \neq 0$ is topic of ongoing research.

4 Energy norm error estimate (stability estimate)

In this section first we give a proof of energy estimate, for the vector $E \in H^2(\Omega_T)$ of the continuous model problem (6). Then we formulate stability estimate for semi-discrete problem which is consequence of the energy estimate for the continuous problem.

Theorem 4.1. *Assume that condition (2) on the functions $\varepsilon(x), \sigma(x)$ hold. Let $\Omega \subset \mathbb{R}^3$ be a bounded domain with the piecewise smooth boundary $\partial\Omega$. For any $t^* \in (0,T)$ let $\Omega_{t^*} = \Omega \times (0,t^*)$ and $\Gamma_{t^*} = \Gamma \times (0,t^*)$. Suppose that there exists a solution $E \in H^2(\Omega_T)$ of the model problem* (6)*. Then the vector E is unique and there exists a constant $C = C(\|\varepsilon\|_{C^2(\Omega)}, \|\sigma\|, t^*)$ such that the following energy estimate is true for all $\varepsilon \geq 1$ in* (6)*:*

$$\begin{aligned} |||E|||^2(t^*) &:= \|\partial_t E\|_{\varepsilon}^2(t^*) + \|E\|_{\sigma}^2(t^*) + \|\nabla E\|^2(t^*) + \|\nabla \cdot E\|_{\varepsilon-1}^2(t^*) \\ &\leq C\left[\|j\|_{\Omega_{t^*}}^2 + \|f_1\|_{\varepsilon}^2 + \|\nabla f_0\|^2 + \|f_0\|_{\sigma}^2 + \|\nabla \cdot f_0\|_{\varepsilon-1}^2\right]. \end{aligned} \tag{17}$$

Proof. We mark the terms in the first line of (6) with

$$\underbrace{\varepsilon\partial_{tt}E}_{\mathbf{I}_1}\underbrace{-\Delta E}_{\mathbf{I}_2}+\underbrace{\nabla(\nabla\cdot((1-\varepsilon)E)}_{\mathbf{I}_3} = \underbrace{-\sigma\partial_t E}_{\mathbf{I}_4} - \underbrace{j}_{\mathbf{I}_5} \tag{18}$$

to simplify notation in our proof, such that $\mathbf{I}_1 + \mathbf{I}_2 + \mathbf{I}_3 = \mathbf{I}_4 + \mathbf{I}_5$.

Through the proof we denote a generic constant of moderate size by $C := C(\|\varepsilon - 1\|_{C^2(\Omega)}, \|\sigma\|_{\infty}, t^*)$. To prove our energy estimate we multiply (18) by $2\partial_t E$ and integrate over Ω_{t^*}, and study it term by term. For the first term in (18) we have

$$\begin{aligned} ((\mathbf{I}_1, 2\partial_t E))_{\Omega_{t^*}} &= ((2\partial_{tt}E, \partial_t E))_{\varepsilon,\Omega_{t^*}} \\ &= \int_0^{t^*} \partial_t \|\partial_t E\|_{\varepsilon}^2(t)\,dt \\ &= \|\partial_t E\|_{\varepsilon}^2(t^*) - \|f_1\|_{\varepsilon}^2 \end{aligned} \tag{19}$$

where we used the chain rule, fundamental theorem of calculus and boundary conditions of (6).

Next we have that

$$((\mathbf{I}_2, 2\partial_t E))_{\Omega_{t^*}} = -((\Delta E, 2\partial_t E))_{\Omega_{t^*}}$$

$$
\begin{aligned}
&= -2\langle\langle \partial_n E, \partial_t E\rangle\rangle_{\Gamma_{t^*}} + ((2\nabla E, \nabla(\partial_t E)))_{\Omega_{t^*}} \\
&= \int_0^{t^*} \partial_t \|\nabla E\|^2(t)\, dt \\
&= \|\nabla E\|^2(t^*) - \|\nabla f_0\|^2 \qquad (20)
\end{aligned}
$$

where we use spatial integration by part, boundary conditions and that $\|\partial_n E\|_{\Gamma_{t^*}} = 0$.

For the third term in (18) we integrate by parts spatially twice and get

$$
\begin{aligned}
((\mathbf{I}_3, 2\partial_t E))_{\Omega_{t^*}} &= ((\nabla(\nabla\cdot((1-\varepsilon)E), 2\partial_t E))_{\Omega_{t^*}} \\
&= 2\langle\langle n\cdot(\nabla\cdot((1-\varepsilon)E), \partial_t E\rangle\rangle_{\Gamma_{t^*}} - 2((\nabla\cdot((1-\varepsilon)E), \nabla\cdot\partial_t E))_{\Omega_{t^*}} \\
&= -2((\nabla(1-\varepsilon)\cdot E, \nabla\cdot\partial_t E))_{\Omega_{t^*}} + ((2\nabla\cdot E, \nabla\cdot\partial_t E))_{\varepsilon-1,\Omega_{t^*}} \\
&= -2\langle\langle\nabla(1-\varepsilon)\cdot E, n\cdot\partial_t E\rangle\rangle_{\Gamma_{t^*}} + 2((\nabla(\nabla(1-\varepsilon)\cdot E), \partial_t E))_{\Omega_{t^*}} \\
&\quad + \int_0^{t^*} \partial_t \|\nabla\cdot E\|^2_{\varepsilon-1}(t)\, dt \\
&= 2((\nabla(\nabla(1-\varepsilon)\cdot E), \partial_t E))_{\Omega_{t^*}} + \|\nabla\cdot E\|^2_{\varepsilon-1}(t^*) - \|\nabla\cdot f_0\|^2_{\varepsilon-1} \qquad (21)
\end{aligned}
$$

Above we made use of (2) (note that since $\varepsilon \equiv 1$ on a neighbourhood of Γ, we have $(1-\varepsilon)|_\Gamma \equiv 0$ and $\nabla(1-\varepsilon)|_\Gamma \equiv 0$). We also made use of the fact that $\nabla\cdot((1-\varepsilon)E) = \nabla(1-\varepsilon)E + (1-\varepsilon)\nabla\cdot E$.

Before estimating the fourth term in (18) we first note that

$$
E(x,t^*) = E(x,0) + \int_0^{t^*} \partial_t E(x,t)\, dt,
$$

and using that $(a+b)^2 \le 2a^2 + 2b^2$ we get

$$
E^2(x,t^*) \le 2E^2(x,0) + 2\Big(\int_0^{t^*} \partial_t E(x,t)\, dt\Big)^2 \le 2E^2(x,0) + 2\int_0^{t^*} (\partial_t E)^2(x,t)\, dt.
$$

If we then integrate these terms over Ω we arrive at

$$
-2((\partial_t E, \partial_t E))_{\Omega_{t^*}} \le -\|E\|^2(t^*) + 2\|E\|^2(0) = \|E\|^2(t^*) + 2\|f_0\|^2.
$$

Applying this to our case we have that

$$
\begin{aligned}
((\mathbf{I}_4, 2\partial_t E))_{\Omega_{t^*}} &= -2((\partial_t E, \partial_t E))_{\sigma,\Omega_{t^*}} \\
&\le -\|E\|^2_\sigma(t^*) + 2\|f_0\|^2_\sigma \qquad (22)
\end{aligned}
$$

For our final term in (18), we simply use that $2ab \le a^2 + b^2$:

$$
((\mathbf{I}_5, 2\partial_t E))_{\Omega_{t^*}} \le ((|j|, 2|\partial_t E|))_{\Omega_{t^*}} \le \|j\|^2_{\Omega_{t^*}} + \|\partial_t E\|^2_{\Omega_{t^*}} \qquad (23)
$$

Next we collect all the terms (19)-(23) to arrive at

$$
\begin{aligned}
&\|\partial_t E\|^2_\varepsilon(t^*) + \|\nabla E\|^2(t^*) + \|\nabla\cdot E\|^2_{\varepsilon-1}(t^*) + \|E\|^2_\sigma(t^*), \\
&\le \|f_1\|^2_\varepsilon + \|\nabla f_0\|^2 + \|\nabla\cdot f_0\|^2_{\varepsilon-1} + 2\|f_0\|^2_\sigma + \|j\|^2_{\Omega_{t^*}} + \|\partial_t E\|^2_{\Omega_{t^*}}
\end{aligned}
$$

$$+2((\nabla(\nabla(\varepsilon-1)\cdot E),\partial_t E))_{\Omega_{t^*}}. \tag{24}$$

We may estimate the last term of (24) using that

$$|\nabla(\nabla(\varepsilon-1)\cdot E)| \leq C(|E|+|\nabla E|).$$

Thus, the above estimate together with the inequality $ab \leq \frac{a^2}{2}+\frac{b^2}{2}$ yields

$$\begin{aligned}
2((|\nabla(\nabla(\varepsilon-1)\cdot E)|,|\partial_t E|))_{\Omega_{t^*}} &\leq 2C((|E|+|\nabla E|,|\partial_t E|))_{\Omega_{t^*}} \\
&\leq C(\|(|E|+|\nabla E|)\|^2_{\Omega_{t^*}}+\|\partial_t E\|^2_{\Omega_{t^*}}) \\
&\leq C(\|E\|^2_{\Omega_{t^*}}+\|\nabla E\|^2_{\Omega_{t^*}}+\|\partial_t E\|^2_{\Omega_{t^*}}).
\end{aligned}$$

Now we can rewrite (24) as

$$\begin{aligned}
F(t^*) &\leq g(t^*)+C(\|\partial_t E\|^2_{\Omega_{t^*}}+\|\nabla E\|^2_{\Omega_{t^*}}+\|E\|^2_{\Omega_{t^*}}) \\
&\leq g(t^*)+C(\|\partial_t E\|^2_{\varepsilon,\Omega_{t^*}}+\|\nabla E\|^2_{\Omega_{t^*}}+\|\nabla\cdot E\|^2_{\varepsilon-1,\Omega_{t^*}}+\|E\|^2_{\sigma,\Omega_{t^*}}) \\
&= g(t^*)+C\int_0^{t^*} F(t)\,dt,
\end{aligned}$$

for some constant $C>0$, where

$$\begin{aligned}
F(t) &:= \|\partial_t E\|^2_{\varepsilon}(t)+\|\nabla E\|^2(t)+\|\nabla\cdot E\|^2_{\varepsilon-1}(t)+\|E\|^2_{\sigma}(t), \\
g(t) &:= \|f_1\|^2_{\varepsilon}+\|\nabla f_0\|^2+\|\nabla\cdot f_0\|^2_{\varepsilon-1}+2\|f_0\|^2_{\sigma}+\int_0^{t^*}\|j\|^2\,dt.
\end{aligned}$$

One application of Grönwall's inequality now gives us the result in (17). □

The next corollary follows from the stability estimate for the continuous problem where all components of the electric field E are replaced with their approximations E_h, as well as all other continuous functions are replaced with their discrete analogs.

Corollary 4.1. *Assume that condition (2) on the functions $\varepsilon(x),\sigma(x)$ hold. For any $t^*\in(0,T)$ let $\Omega_{t^*}=\Omega\times(0,t^*)$ and $\Gamma_{t^*}=\Gamma\times(0,t^*)$. Suppose that there exists a solution $E_h\in \boldsymbol{W}_h^E(\Omega)$ of the problem (11) and the approximations of the initial data $f_{0,h}$ and $f_{1,h}$ satisfy the regularity conditions $f_{1,h},f_{0,h}\in\boldsymbol{W}_h^E(\Omega)$. Then E_h is unique and there exists a constant $C=C(\|\varepsilon\|_{C^2(\Omega)},\|\sigma\|,t^*)$ such that the following energy estimate is true for all $\varepsilon\geq 1,\sigma>0,\varepsilon>\sigma$ in (11):*

$$\begin{aligned}
|||E_h|||^2(t^*) &:= \|\partial_t E_h\|^2_{\varepsilon}(t^*)+\|E_h\|^2_{\sigma}(t^*)+\|\nabla E_h\|^2(t^*)+\|\nabla\cdot E_h\|^2_{\varepsilon-1}(t^*) \\
&\leq C\left[\|j\|^2_{\Omega_{t^*}}+\left\|f_{1,h}\right\|^2_{\varepsilon}+\left\|\nabla f_{0,h}\right\|^2+\left\|f_{0,h}\right\|^2_{\sigma}+\left\|\nabla\cdot f_{0,h}\right\|^2_{\varepsilon-1}\right].
\end{aligned} \tag{25}$$

5 A priori error estimates

In this section we present an *a priori error* estimate for the error $e = E(\cdot,t) - E_h(\cdot,t)$ between the solution E of the model problem (6) and solution E_h of the semi-discretized problem (11).

Let

$$e := E(\cdot,t) - E_h(\cdot,t) = E - \Pi_h E + \Pi_h E - E_h = \eta + \xi, \qquad (26)$$

where $\eta := E - \Pi_h E$, $\xi := \Pi_h E - E_h$. Here, $\Pi_h E : \mathbf{H}^1_E(\Omega_T) \longrightarrow \mathbf{W}^E_h(\Omega_T)$ is an elliptic projection operator for $E \in H(div, \Omega)$, see details in [1, 20], such that $\forall \mathbf{v} \in \mathbf{W}^E_h(\Omega)$

$$a(\Pi_h E, \mathbf{v}) = a(E, \mathbf{v}). \qquad (27)$$

The first part of error, $\eta = E - \Pi_h E$, can be estimated as follows.

Theorem 5.1. *Let $E \in \boldsymbol{H}^2_E(\Omega_T)$ bet the solution of the continuous problem* (6)*. Then*

$$\begin{aligned} ||\eta||_{L_2} &\leq C_I(\tau^2||D_t^2 E|| + h^2||D_x^2 E||), \\ ||\eta||_{H^1} &\leq C_I(\tau||D_t^2 E|| + h||D_x^2 E||). \end{aligned} \qquad (28)$$

For semi-discretized problem (11) *these estimates reduces to:*

$$\begin{aligned} ||\eta||_{L_2} &\leq C_I h^2||D_x^2 E||, \\ ||\eta||_{H^1} &\leq C_I h||D_x^2 E||. \end{aligned} \qquad (29)$$

Proof. We observe that using (27) we can get $\forall v \in \mathbf{W}^E_h(\Omega_T)$

$$\begin{aligned} \|\eta\|^2 = \|E - \Pi_h E\|^2 &= (E - \Pi_h E, E - \Pi_h E) \\ &= (E - \Pi_h E, E - v) + (E - \Pi_h E, v - \Pi_h E) \\ &= (E - \Pi_h E, E - v) \leq \|E - \Pi_h E\| \|E - v\|, \end{aligned} \qquad (30)$$

and thus,

$$\|\eta\| = \|E - \Pi_h E\| \leq \|E - v\|. \qquad (31)$$

Taking $v = E_h^I$ in (31) , where E_h^I is nodal interpolant of E, and using standard interpolation error estimates [20, 30, 12] for the fully discrete scheme in space and time we get

$$\begin{aligned} \|\eta\|_{L_2} &\leq C_I(\tau^2||D_t^2 E|| + h^2||D_x^2 E||), \\ ||\eta||_{H^1} &\leq C_I(\tau||D_t^2 E|| + h||D_x^2 E||), \end{aligned} \qquad (32)$$

where C_I are interpolation constants. For semi-discretized problem (11) terms with $D_t^2 E$ disappear and these estimates reduces to (29).

□

In the proof of a priori error estimate we use the constant C as a moderate constant which is adjusted throughout the proof, as well as well-posedness of the bilinear form $a(\cdot,\cdot)$. Let us briefly sketch the proof of well-posedness of $a(\cdot,\cdot)$. We refer to [4] for the full details of this proof.

Let us define the linear form as

$$\mathscr{L}(\mathbf{v}) := -(j,v). \tag{33}$$

We now can rewrite the equation (11) as

$$(\varepsilon\partial_{tt}E_h,\mathbf{v})+(\sigma\partial_t E_h,\mathbf{v})+a(E_h,\mathbf{v}) = \mathscr{L}(\mathbf{v}). \tag{34}$$

Theorem 5.2 (well-posedness of $a(\cdot,\cdot)$)**.** *Assume that the following condition holds*

$$|\nabla\varepsilon| \leq \frac{1}{2}\min(1/2,\varepsilon-1). \tag{35}$$

Let

$$|||E_h|||_a^2 :=\| E_h \|_\varepsilon^2 + \| \nabla E_h \|^2 + \| \nabla\cdot E_h \|_{\varepsilon-1}^2 . \tag{36}$$

Then for all E_h and $\boldsymbol{v} \in \boldsymbol{W}_h^E(\Omega)$ the discrete bilinear form $a(\cdot,\cdot)$ is well-posed, or:

$$a(E_h,E_h) \geq \frac{1}{2}|||E_h|||_a^2 \qquad \textit{(Coercivity of a)}, \tag{37}$$

$$a(E_h,\boldsymbol{v}) \leq C_2|||E_h|||_a\,|||\boldsymbol{v}|||_a, \qquad \textit{(Continuity of a)}, \tag{38}$$

$$|\mathscr{L}(\boldsymbol{v})| \leq C_3|||\boldsymbol{v}|||_a, \qquad \textit{(Continuity of } \mathscr{L}\textit{)}. \tag{39}$$

where, $C_i, i=2,3$ are positive constants.

Proof. We use a Lax-Milgram approach, or we will show that the discrete bilinear form $a(\cdot,\cdot)$ is coercive, and both $a(\cdot,\cdot)$ and $\mathscr{L}(\cdot)$ are continuous.

To prove coercivity of $a(\cdot,\cdot)$ we choose $\mathbf{v} = E_h$ in (13) to get

$$\begin{aligned} a(E_h,E_h) &= (\nabla E_h,\nabla E_h)+(\nabla(\varepsilon-1)E_h,\nabla\cdot E_h)+((\varepsilon-1)\nabla\cdot E_h,\nabla\cdot E_h)\\ &=\| \nabla E_h \|^2 + \| \nabla\cdot E_h \|_{\varepsilon-1}^2 +(\nabla(\varepsilon-1)E_h,\nabla\cdot E_h). \end{aligned} \tag{40}$$

In (40) we have used the equality

$$(\nabla\cdot((\varepsilon-1)E_h),\nabla\cdot\mathbf{v}) = (\nabla(\varepsilon-1)E_h+(\varepsilon-1)\nabla\cdot E_h,\nabla\cdot\mathbf{v}). \tag{41}$$

Since $\nabla(\varepsilon-1) = \nabla\varepsilon$ we can use the following estimate derived in [4]:

$$\pm\Big((\nabla\varepsilon)E_h,\nabla\cdot E_h\Big) \geq -\frac{1}{2}\,\|E_h\|_{|\nabla\varepsilon|}^2 - \frac{1}{2}\,\|\nabla\cdot E_h\|_{|\nabla\varepsilon|}^2\,, \tag{42}$$

Using (42) and assumption (35) we obtain coercivity of a:

$$\begin{aligned} a(E_h,E_h) &=\| \nabla E_h \|^2 + \| \nabla\cdot E_h \|_{\varepsilon-1}^2 +(\nabla(\varepsilon-1)E_h,\nabla\cdot E_h)\\ &\geq\| \nabla E_h \|^2 + \| \nabla\cdot E_h \|_{\varepsilon-1}^2 -\frac{1}{2}\,\|E_h\|_{|\nabla\varepsilon|}^2 - \frac{1}{2}\,\|\nabla\cdot E_h\|_{|\nabla\varepsilon|}^2 \geq \frac{1}{2}|||E_h|||_a^2. \end{aligned} \tag{43}$$

To prove continuity of $a(\cdot,\cdot)$, we use *Cauchy-Schwarz' inequality* and estimate (42) to obtain $\forall \mathbf{v} \in \mathbf{W}_h^E(\Omega)$:

$$\begin{aligned} a(E_h, \mathbf{v}) &= (\nabla E_h, \nabla \mathbf{v}) + (\nabla \cdot ((\varepsilon - 1)E_h), \nabla \cdot \mathbf{v}) \\ &= (\nabla E_h, \nabla \mathbf{v}) + ((\varepsilon - 1)\nabla \cdot E_h, \nabla \cdot \mathbf{v}) + ((\nabla \varepsilon)E_h, \nabla \cdot \mathbf{v}) \\ &\leq \| \nabla E_h \| \| \nabla \mathbf{v} \| + \| \nabla \cdot E_h \|_{\varepsilon-1} \| \nabla \cdot \mathbf{v} \|_{\varepsilon-1} \\ &+ \| E_h \|_{|\nabla\varepsilon|} \| \nabla \cdot \mathbf{v} \|_{|\nabla\varepsilon|} \leq C|||E_h|||_a \cdot |||\mathbf{v}|||_a. \end{aligned} \tag{44}$$

Finally, we can verify continuity of $\mathscr{L}(\mathbf{v})$:

$$|\mathscr{L}(\mathbf{v})| = |(-j, \mathbf{v})| \leq \| j \| \| \mathbf{v} \| \leq \| j \| \, |||\mathbf{v}|||. \tag{45}$$

□

Theorem 5.3. *Let $E \in \boldsymbol{H}_E^2(\Omega_T)$ solves the continuous problem* (6)*, and $E_h \in \mathbf{W}_h^E(\Omega_T)$ solves the semi-discretized problem* (11)*. Assume that $E(t), \partial_t E(t), \partial_{tt} E(t) \in H^2(\Omega)$. Further assume that the assumptions* (2) *and* (35) *on functions ε and σ hold, as well as $f_0, f_1 \in [H^1(\Omega)]^3$, $f_{0h}, f_{1h}, j_h \in [W_h^E(\Omega)]^3$ and $j \in [L^2(\Omega_T)]^3$. Then there exists a constant $C(\varepsilon,\sigma)$ such that for all $t \in [0,T]$ the following a priori error estimates hold:*

$$\begin{aligned} \|e(t)\| &= ||E(\cdot,t) - E_h(\cdot,t)|| \leq C_I h^2 (\|D_x^2 E\|_\Omega + 2d_1 t \int_0^T (\|\partial_{ss} D_x^2 E\|_\Omega + \|\partial_s D_x^2 E\|_\Omega)\, ds), \\ \|e(t)\|_{H^1} &= ||E(\cdot,t) - E_h(\cdot,t)||_{H^1} \leq C_I h (\|D_x^2 E\|_\Omega + 2d_1 t \int_0^T (\|\partial_{ss} D_x^2 E\|_\Omega + \|\partial_s D_x^2 E\|_\Omega)\, ds). \end{aligned} \tag{46}$$

Proof. Since η is estimated via standard interpolation error estimates (28), we begin to estimate ξ. We first note that $\forall \mathbf{v} \in \mathbf{W}_h^E(\Omega)$

$$\begin{aligned} a(\Pi_h E, \mathbf{v}) &= a(E, \mathbf{v}) \\ &= -(j, \mathbf{v}) - (\varepsilon \partial_{tt} E, \mathbf{v}) - (\sigma \partial_t E, \mathbf{v}) \\ &+ (\varepsilon \partial_{tt} \Pi_h E, \mathbf{v}) + (\sigma \partial_t \Pi_h E, \mathbf{v}) - (\varepsilon \partial_{tt} \Pi_h E, \mathbf{v}) - (\sigma \partial_t \Pi_h E, \mathbf{v}). \end{aligned} \tag{47}$$

Using (26) the equation above can be rewritten as

$$(\varepsilon \partial_{tt} \Pi_h E, \mathbf{v}) + (\sigma \partial_t \Pi_h E, \mathbf{v}) + a(\Pi_h E, \mathbf{v}) = -(j, \mathbf{v}) - (\varepsilon \partial_{tt} \eta, \mathbf{v}) - (\sigma \partial_t \eta, \mathbf{v}). \tag{48}$$

By subtracting the first equation of (11) from the expression above, while letting $\mathbf{v} := \partial_t \xi$ we arrive at

$$(\varepsilon \partial_{tt} \xi, \partial_t \xi) + (\sigma \partial_t \xi, \partial_t \xi) + a(\xi, \partial_t \xi) = -(\varepsilon \partial_{tt} \eta, \partial_t \xi) - (\sigma \partial_t \eta, \partial_t \xi). \tag{49}$$

Note that $\forall \mathbf{v} \in \mathbf{W}_h^E(\Omega)$

$$a(\xi, \mathbf{v}) = a(\Pi_h E - E_h, \mathbf{v}) = a(E - E_h, \mathbf{v}) = 0,$$

by the properties of Π_h and Galerkin orthogonality. Using this we observe that in (49) the term $a(\xi,\partial_t\xi)=0$. Thus, we can estimate a lower bound of the left-hand side of (49) as

$$(\varepsilon\partial_{tt}\xi,\partial_t\xi)+(\sigma\partial_t\xi,\partial_t\xi)+a(\xi,\partial_t\xi)\geq(\varepsilon\partial_{tt}\xi,\partial_t\xi)=\frac{1}{2}\partial_t\|\varepsilon\partial_t\xi\|_\Omega^2\geq\frac{1}{2}\partial_t\|\partial_t\xi\|_\Omega^2, \tag{50}$$

where we have used that $(\sigma\partial_t\xi,\partial_t\xi)\geq 0$ and $\varepsilon\geq 1,\sigma\geq 0$.

We can also estimate an upper bound for the right-hand side of (49):

$$-(\varepsilon\partial_{tt}\eta,\partial_t\xi)-(\sigma\partial_t\eta,\partial_t\xi)\leq(\|\varepsilon\partial_{tt}\eta\|_\Omega+\|\sigma\partial_t\eta\|_\Omega)\|\partial_t\xi\|_\Omega. \tag{51}$$

Collecting these two estimates, we have

$$\partial_t\|\partial_t\xi\|_\Omega^2\leq 2(\|\varepsilon\partial_{tt}\eta\|_\Omega+\|\sigma\partial_t\eta\|_\Omega)\|\partial_t\xi\|_\Omega. \tag{52}$$

Integrating over $[0,t^*]$ where $t^*\in[0,T]$ and using conditions (2) for functions ε,σ noting that $\varepsilon>\sigma$ we get

$$\begin{aligned}\|\partial_t\xi\|_\Omega^2(t^*)&\leq 2\int_0^{t^*}(\|\varepsilon\partial_{ss}\eta\|_\Omega+\|\sigma\partial_s\eta\|_\Omega)\|\partial_s\xi\|_\Omega(s)\,ds\\&\leq 2d_1\int_0^{t^*}(\|\partial_{ss}\eta\|_\Omega+\|\partial_s\eta\|_\Omega)(s)\,ds\cdot\max_{t'\in[0,T]}\|\partial_s\xi\|_\Omega,\end{aligned} \tag{53}$$

where we have used that $\xi(\cdot,0)=\partial_t\xi(\cdot,0)=0$, and $\sigma\leq\varepsilon\leq d_1$.

Since (53) holds for all $t^*\in[0,T]$, we have

$$\begin{aligned}&\max_{t'\in[0,T]}\|\partial_t\xi\|_\Omega^2\leq 2d_1\int_0^T(\|\partial_{ss}\eta\|_\Omega+\|\partial_s\eta\|_\Omega)(s)\,ds\cdot\max_{t'\in[0,T]}\|\partial_t\xi\|_\Omega,\\&\max_{t'\in[0,T]}\|\partial_t\xi\|_\Omega\leq 2d_1\int_0^T(\|\partial_{ss}\eta\|_\Omega+\|\partial_s\eta\|_\Omega)(s)\,ds.\end{aligned} \tag{54}$$

Substituting this estimate into (53), we finally obtain

$$\|\partial_t\xi\|_\Omega\leq 2d_1\int_0^T(\|\partial_{ss}\eta\|_\Omega+\|\partial_s\eta\|_\Omega)(s)\,ds. \tag{55}$$

To proceed further we use estimate (28) to get

$$\int_0^{t^*}(\|\partial_{ss}\eta\|_\Omega+\|\partial_s\eta\|_\Omega)(s)\,ds\leq C_I h^2\int_0^T(\|\partial_{ss}D_x^2E\|_\Omega+\|\partial_sD_x^2E\|_\Omega)\,ds. \tag{56}$$

Using (56) in (55) we obtain

$$\|\partial_t\xi\|_\Omega\leq 2d_1C_Ih^2\int_0^T(\|\partial_{ss}D_x^2E\|_\Omega+\|\partial_sD_x^2E\|_\Omega)\,ds. \tag{57}$$

Further, we observe that

$$\begin{aligned}\frac{d}{dt}\|\xi\|_\Omega^2=2\|\xi\|_\Omega\frac{d}{dt}\|\xi\|_\Omega&=\frac{d}{dt}\int_\Omega|\xi|^2\,dx\\&=2\int_\Omega\xi\cdot\xi_t\,dx\leq 2\|\xi\|_\Omega\|\partial_t\xi\|_\Omega\end{aligned} \tag{58}$$

from which it follows that

$$\frac{d}{dt} \|\xi\|_\Omega \leq \|\partial_t \xi\|_\Omega . \tag{59}$$

Integrating in time (59) and using (57) yields

$$\|\xi(t)\|_\Omega \leq \int_0^t \|\partial_s \xi\|_\Omega \, ds \leq 2 d_1 C_I h^2 t \int_0^T (\|\partial_{ss} D_x^2 E\|_\Omega + \|\partial_s D_x^2 E\|_\Omega) \, ds \tag{60}$$

From (60) and (28) follows also that

$$\|\xi(t)\|_{H^1} \leq 2 d_1 C_I h t \int_0^T (\|\partial_{ss} D_x^2 E\|_\Omega + \|\partial_s D_x^2 E\|_\Omega) \, ds. \tag{61}$$

Summing up (28), (60) and (61) we get the desired error estimates (46), and the proof is complete.

□

6 Numerical examples

In this section we perform computations which will confirm theoretical predictions given in Theorem 4. All computations are performed in the software package WavES [41] using C++/PETSC [38]. The computational domain $\Omega \times (0,T)$ is chosen as $\Omega = [0,1] \times [0,1]$ with $\Omega_1 = [0.25, 0.75] \times [0.25, 0.75]$ such that $\Omega_1 \subset \Omega$. To discretize the computational domain Ω we denote by $\mathscr{T}_{hl} := \{K\}$ a partition of the domain Ω into triangles K of sizes $h_l = 2^{-l}, l = 3, ..., 6$. The explicit finite element scheme (15) derived in [9] was used in computations. We have chosen the time step $\tau = 0.0005$ such that the whole explicit scheme remains stable.

We have used following time-dependent model problem in computations:

$$\begin{aligned} \varepsilon(\mathbf{x}) \frac{\partial^2 E(\mathbf{x},t)}{\partial t^2} + \nabla \times \nabla \times E(\mathbf{x},t) + \sigma(\mathbf{x}) \frac{\partial E(\mathbf{x},t)}{\partial t} &= f(\mathbf{x},t), \\ \nabla \cdot (\varepsilon E)(\mathbf{x},t) &= 0, \\ E(\mathbf{x},0) = 0, \quad \frac{\partial E}{\partial t}(\mathbf{x},0) &= 0, \\ E|_\Gamma &= 0. \end{aligned} \tag{62}$$

The source data $f(\mathbf{x},t)$, $\mathbf{x} := (x,y) \in \mathbb{R}^2$, $t \in [0, 0.25]$ is computed by knowing the exact solution

$$\begin{aligned} E_1(\mathbf{x},t) &= \frac{t^2}{\varepsilon} \pi \sin^2 \pi x \cos \pi y \sin \pi y, \\ E_2(\mathbf{x},t) &= -\frac{t^2}{\varepsilon} \pi \sin^2 \pi y \cos \pi x \sin \pi x \end{aligned} \tag{63}$$

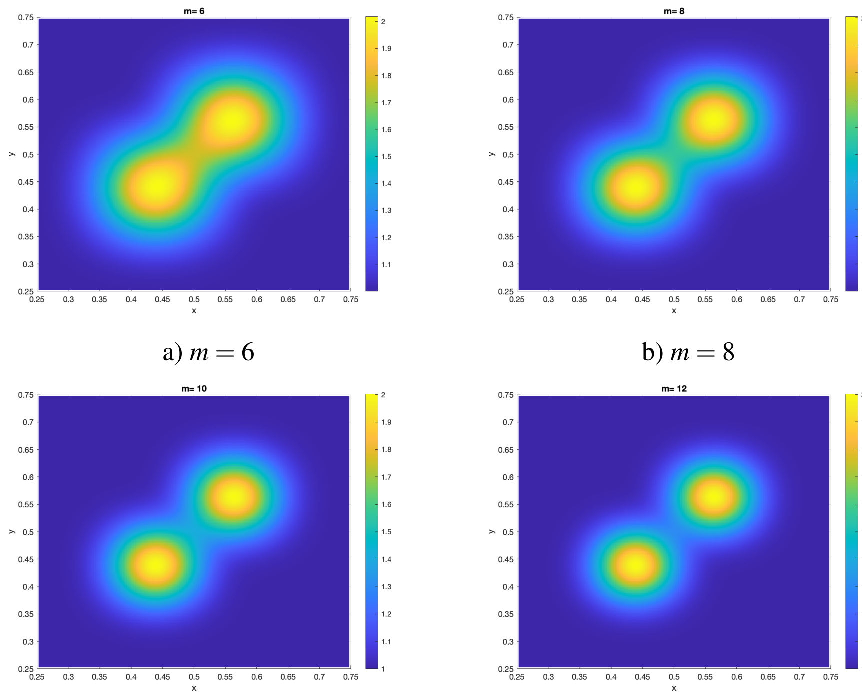

a) $m = 6$ b) $m = 8$

c) $m = 10$ d) $m = 12$

Figure 1: a) The function $\varepsilon(x,y)$ in the domain $\Omega_1 = [0.25, 0.75] \times [0.25, 0.75]$ for different values of m in (64)

.

of the problem (62).

In the model problem (62) the function $\varepsilon(x,y)$ is defined as

$$\varepsilon(x,y) = \begin{cases} 1 & +(\sin\pi(2x-0.375))^m \cdot (\sin\pi(2y-0.375))^m \\ & +(\sin\pi(2x-0.625))^m \cdot (\sin\pi(2y-0.625))^m \quad \text{in } \Omega_1, \\ 1 & \quad \text{otherwise,} \end{cases} \tag{64}$$

and the function $\sigma(x,y)$ as

$$\sigma(x,y) = \begin{cases} 0.001(1 & +(\sin\pi(2x-0.375))^m \cdot (\sin\pi(2y-0.375))^m \\ & +(\sin\pi(2x-0.625))^m \cdot (\sin\pi(2y-0.625))^m) \quad \text{in } \Omega_1, \\ 0 & \quad \text{otherwise} \end{cases} \tag{65}$$

Figures 1, 2 show the functions ε and σ, respectively, for different $m = 6, 8, 10, 12$ in (64), (65) which were used in computations.

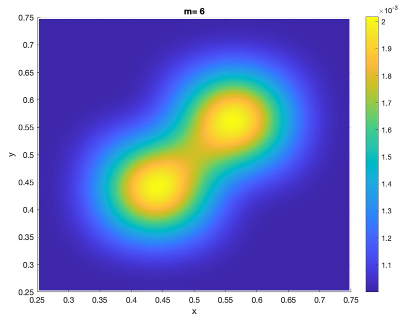

a) $m = 6$

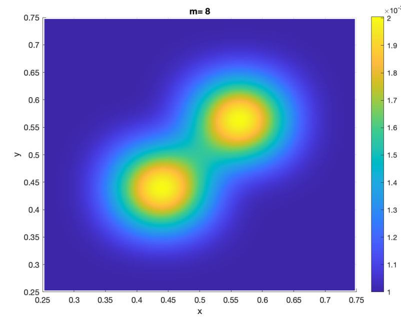

b) $m = 8$

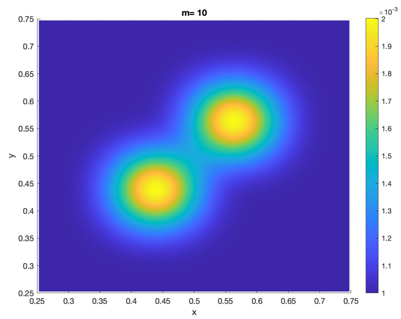

c) $m = 10$

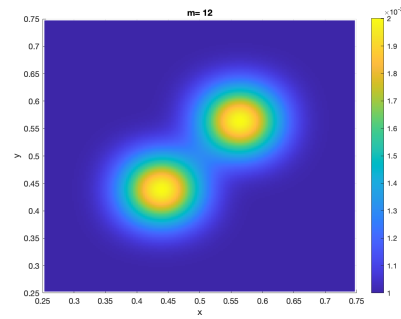

d) $m = 12$

Figure 2: a) The function $\sigma(x,y)$ in the domain $\Omega_1 = [0.25, 0.75] \times [0.25, 0.75]$ for different values of m in (64)

.

Relative errors $\Theta^{(1)}, \Theta^{(2)}$ are computed at the time moment $t = 0.25$ as

$$\Theta^{(1)} = \frac{\|\hat{E} - \hat{E}_h\|_{L_2}}{\|\hat{E}\|_{L_2}}, \qquad \text{and} \tag{66}$$

$$\Theta^{(2)} = \frac{\|\nabla(\hat{E} - \hat{E}_h)\|_{L_2}}{\|\nabla\hat{E}\|_{L_2}}, \tag{67}$$

in L_2- and H^1-norms, respectively. Here, $\hat{E} = (\hat{E}_1, \hat{E}_2)$ is the exact solution given by (63), and $\hat{E}_h = (\hat{E}_{1h}, \hat{E}_{2h})$ is the computed solution. We note also that

$$|\hat{E}| := \sqrt{\hat{E}_1^2 + \hat{E}_2^2} \qquad |\hat{E}_h| := \sqrt{\hat{E}_{1h}^2 + \hat{E}_{2h}^2}. \tag{68}$$

Figures 3 present convergence results of explicit finite element scheme (15) for the functions ε and σ defined by (64), (65), respectively, for different values of $m = 6, 8, 10, 12$. Table 1, Table 2, Table 3 and Table 4 present relative errors $\Theta_l^{(j)},\ j = 1,2$ and convergence rates $r_l^{(j)},\ j = 1,2$ in the L_2-norm and in the H^1-norm for mesh sizes

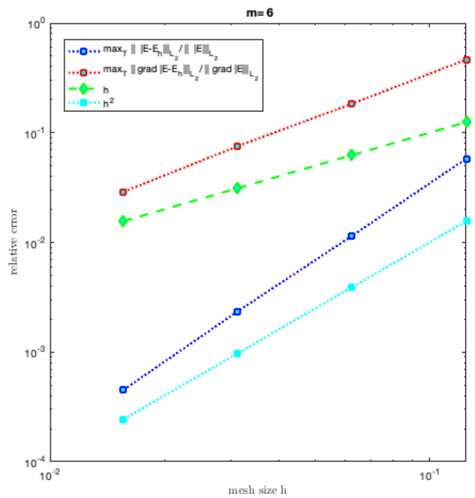

a) $m = 6$

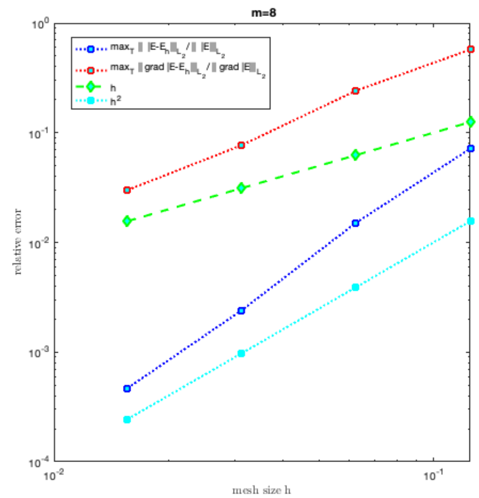

b) $m = 8$

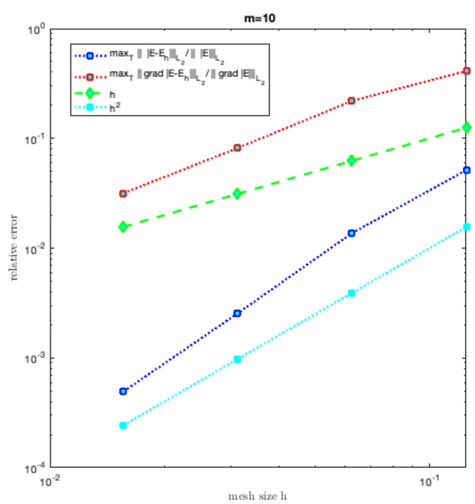

c) $m = 10$

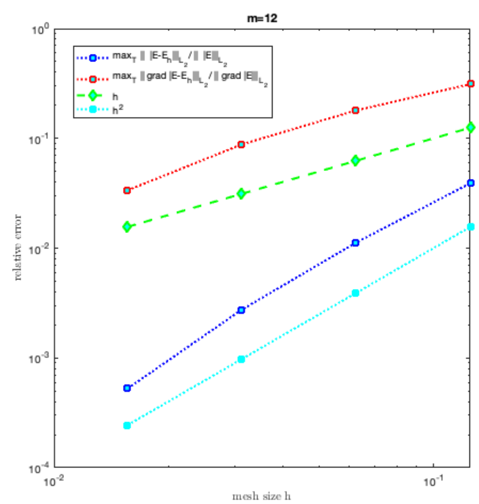

d) $m = 12$

Figure 3: Relative errors for different m in (64), (65)

.

$h_l = 2^{-l}, l = 3, ..., 6$, for different values of $m = 6, 8, 10, 12$ in (64),(65). We note that chosen values of m satisfy the regularity assumptions on the exact solution, see details in [10].

We used following expressions to compute convergence rates $r^{(1)}$ and $r^{(2)}$ presented in these figures and tables:

$$
\begin{aligned}
r^{(1)} &= \frac{\left|\log\left(\frac{\Theta_l^{(1)}}{\Theta_{l+1}^{(1)}}\right)\right|}{|\log(2)|}, \\
r^{(2)} &= \frac{\left|\log\left(\frac{\Theta_l^{(2)}}{\Theta_{l+1}^{(2)}}\right)\right|}{|\log(2)|},
\end{aligned}
\tag{69}
$$

where $\Theta_l^{(j)},\ j=1,2$ are computed relative norms $\Theta^{(j)},\ j=1,2$ on the mesh $\mathscr{T}_h$ with the mesh sizes $h_l = 2^{-l}, l = 3,...,5$.

l	nel	nno	$\Theta^{(1)}$	$\frac{\Theta_l^{(1)}}{\Theta_{l+1}^{(1)}}$	$r^{(1)}$	$\Theta^{(2)}$	$\frac{\Theta_l^{(2)}}{\Theta_{l+1}^{(2)}}$	$r^{(2)}$
3	128	81	0.058066	-	-	0.464524	-	-
4	512	289	0.011481	5.057543	2.34	0.183696	2.528771	1.34
5	2048	1089	0.002355	4.875048	2.29	0.075362	2.437524	1.29
6	8192	4225	0.000453	5.202624	2.38	0.028971	2.601312	1.38

Table 1: Relative errors $\Theta_l^{(j)},\ j=1,2$ and convergence rates $r_l^{(j)},\ j=1,2$ in the L_2-norm and in the H^1-norm for mesh sizes $h_l = 2^{-l}, l = 3,...,6$, for $m = 6$ in (64),(65).

l	nel	nno	$\Theta^{(1)}$	$\frac{\Theta_l^{(1)}}{\Theta_{l+1}^{(1)}}$	$r^{(1)}$	$\Theta^{(2)}$	$\frac{\Theta_l^{(2)}}{\Theta_{l+1}^{(2)}}$	$r^{(2)}$
3	128	81	0.071545	-	-	0.572362	-	-
4	512	289	0.015110	4.735050	2.24	0.241756	2.367525	1.24
5	2048	1089	0.002406	6.280222	2.65	0.076989	3.140111	1.65
6	8192	4225	0.000469	5.130590	2.36	0.030012	2.565295	1.36

Table 2: Relative errors $\Theta_l^{(j)},\ j=1,2$ and convergence rates $r_l^{(j)},\ j=1,2$ in the L_2-norm and in the H^1-norm for mesh sizes $h_l = 2^{-l}, l = 3,...,6$, for $m = 8$ in (64), (65).

Using Figures 3 and tables we observe that the explicit finite element scheme derived in [9] behaves like a first order method in in $H^1(\Omega)$-norm and second order method in $L_2(\Omega)$-norm. Therefore, these results confirm theoretical analytic estimates derived in Theorem 4.

7 Conclusions

This paper presents stability and convergence analysis for the finite element method for stabilized time-dependent Maxwell's equations in conductive nonmagnetic media

l	nel	nno	$\Theta^{(1)}$	$\frac{\Theta_l^{(1)}}{\Theta_{l+1}^{(1)}}$	$r^{(1)}$	$\Theta^{(2)}$	$\frac{\Theta_l^{(2)}}{\Theta_{l+1}^{(2)}}$	$r^{(2)}$
3	128	81	0.051348	-	-	0.410785	-	-
4	512	289	0.013703	3.747278	1.91	0.219245	1.873639	0.91
5	2048	1089	0.002553	5.367863	2.42	0.081688	2.683932	1.42
6	8192	4225	0.000495	5.156936	2.37	0.031681	2.578468	1.37

Table 3: Relative errors $\Theta_l^{(j)},\ j=1,2$ and convergence rates $r_l^{(j)},\ j=1,2$ in the L_2-norm and in the H^1-norm for mesh sizes $h_l = 2^{-l}, l = 3,...,6$, for $m = 10$ in (64), (65).

l	nel	nno	$\Theta^{(1)}$	$\frac{\Theta_l^{(1)}}{\Theta_{l+1}^{(1)}}$	$r^{(1)}$	$\Theta^{(2)}$	$\frac{\Theta_l^{(2)}}{\Theta_{l+1}^{(2)}}$	$r^{(2)}$
3	128	81	0.038995	-	-	0.311959	-	-
4	512	289	0.011230	3.472240	1.80	0.179688	1.736128	0.80
5	2048	1089	0.002753	4.078874	2.03	0.088106	2.039437	1.03
6	8192	4225	0.000526	5.238828	2.39	0.033636	2.619414	1.39

Table 4: Relative errors $\Theta_l^{(j)},\ j=1,2$ and convergence rates $r_l^{(j)},\ j=1,2$ in the L_2-norm and in the H^1-norm for mesh sizes $h_l = 2^{-l}, l = 3,...,6$, for $m = 12$ in (64), (65).

developed in [9]. We present analysis for a specific case when the dielectric permittivity and conductivity functions have a constant value in a boundary neighborhood.

In the theoretical part of the paper we derived energy norm stability estimates for the continuous and discrete solutions of the model problem, as well as a priori error bounds in the gradient dependent, weighted norms. Our numerical computations confirm theoretical predictions and show that our method behaves like a first order method in $H^1(\Omega)$-norm and second order method in $L_2(\Omega)$-norm.

Acknowledgment The research of both authors is supported by the Swedish Research Council grant VR 2018-03661.

■

References

[1] M. Asadzadeh, *An Introduction to Finite Element Methods for Differential Equations*, Wiley, 2020.

[2] Douglas N. Arnold, Franco Brezzi, Bernardo Cockburn, and L. Dontella Marini, Unified analysis for discontinuous Galerkin methods for elliptic problems, *SIAM J Numer Anal, vol xx, (19xx).*

[3] F. Assous, P. Degond, E. Heinzé, P.-A. Raviart and J. Segré, On finite element method for solving the Three-Dimensional Maxwell Equations. *J. Comput. Phys., 109:222-237, 1993.*

[4] M. Asadzadeh, L. Beilina, A stabilized $P1$ domain decomposition finite element method for time harmonic Maxwell's equations, *Mathematics and Computers in Simulation, 204, 556-574*, (2023)

[5] M. Asadzadeh, M. and L. Beilina, Stability and Convergence Analysis of a Domain Decomposition FE/FD Method for Maxwell's Equations in the Time Domain, *Algorithms* 2022, 15(10), 337; `https://doi.org/10.3390/a15100337`

[6] Baudouin, L.; de Buhan, M.; Ervedoza, S.; Osses, A. Carleman-based reconstruction algorithm for the waves. SIAM J. Numer. Anal. 2020, 59, 998–1039.

[7] L. Beilina, Energy estimates and numerical verification of the stabilized Domain Decomposition Finite Element/Finite Difference approach for time-dependent Maxwell's system, *Cent. Eur. J. Math.*, 11, 702-733, 2013. DOI: 10.2478/s11533-013-0202-3.

[8] L. Beilina, E. Lindström, A posteriori error estimates and adaptive error control for permittivity reconstruction in conductive media. In Gas Dynamics with Applications in Industry and Life Sciences, Series: Springer Proceedings in Mathematics Statistics, Springer, PROMS, vol.429, Cham 2023

[9] L. Beilina, E. Lindström, An adaptive finite element/finite difference domain decomposition method for applications in microwave imaging, Electronics, MDPI, 2022

[10] L. Beilina, V. Ruas, An explicit P1 finite element scheme for Maxwell's equations with constant permittivity in a boundary neighborhood, arXiv:1808.10720.

[11] L. Beilina and M. V. Klibanov, *Approximate global convergence and adaptivity for Coefficient Inverse Problems*, Springer, New York, 2012.

[12] S. C. Brenner and L. R. Scott, *The Mathematical Theory of Finite Element Methods*, Springer-Verlag, Berlin, 1994.

[13] J. Bondestam Malmberg, L. Beilina, An Adaptive Finite Element Method in Quantitative Reconstruction of Small Inclusions from Limited Observations, *Appl. Math. Inf. Sci.*, 12(1), 1-19, 2018.

[14] A. S. Bonnet-Ben Dhia, C. Hazard and S. Lohrengel, A singular field method for the solution of Maxwell's equations in polyhedral domains, *SIAM J. Appl. Math., 59-6. pp. 2028-2044, 1999.*

[15] P. Ciarlet Jr., Augmented formulations for solving Maxwell equations *Computer Methods in Applied Mechanics and Engineering*, 194 (2-5), 2005

[16] P. Ciarlet Jr. and E. Jamelot Continuous Galerkin methods for solving the time-dependent Maxwell equations in 3D geometries *J. Comput. Phys.*, 226 (1), 2007

[17] G. C. Cohen, *Higher Order Numerical Methods for Transient Wave Equations*, Springer-Verlag, Berlin, 2002.

[18] M. Dauge and M. Costabel, Singularities of Maxwell's equations on polyhedral domains, in *Analysis, numerics and applications of differential and integral equations*, M. Bach, C. Constanda, G.C. Hsiao, A.M. Sändig, P. Werner eds. Pitman Research Notes in Mathematics Series, 379, 1998.

[19] M. Dauge and M. Costabel, Weighted Regularization of Maxwell Equations in Polyhedral Domains. A rehabilitation of nodal finite elements, *Numer. Math.*, 93 (2), 2002.

[20] K. Eriksson, D. Estep, P. Hansbo and C. Johnson, Computational Differential Equations, Combridge, 1996.

[21] A. Ern, J.-L. Guermond Analysis of the edge finite element approximation of the Maxwell equations with low regularity solutions. Computers and Mathematics with Applications, 75 (3), 2018

[22] A. Elmkies and P. Joly, Finite elements and mass lumping for Maxwell's equations: the 2D case. *Numerical Analysis*, C. R. Acad.Sci.Paris, 324, pp. 1287–1293, 1997.

[23] L. C. Evans, *Partial Differential Equations*, Amer. Math. Soc., Providence, RI, 1993.

[24] Y. G. Gleichmann and M. J. Grote, Adaptive Spectral Inversion for inverse medium problems, Inverse problems, 39(12), 2023.

[25] Lazebnik, M.; McCartney, L.; Popovic, D.; Watkins, C.B.; Lindstrom, M.J.; Harter, J.; Sewall, S.; Magliocco, A.; Booske, J.H.; Okoniewski, M.; et al. A large-scale study of the ultrawideband microwave dielectric properties of normal breast tissue obtained from reduction surgeries. Phys. Med. Biol. 2007, 52, 2637–2656.

[26] E. Jamelot, *Résolution des équations de Maxwell avec des éléments finis de Galerkin continus* PhD thesis, Ecole Polytechnique, 2005

[27] B. Jiang, *The Least-Squares Finite Element Method. Theory and Applications in Computational Fluid Dynamics and Electromagnetics*, Springer-Verlag, Heidelberg, 1998.

[28] B. Jiang, J. Wu and L. A. Povinelli, The origin of spurious solutions in computational electromagnetics, *Journal of Computational Physics*, 125, 104-123, 1996.

[29] J. Jin, *The finite element method in electromagnetics*, Wiley, 1993.

[30] C. Johnson, *Numerical solutions of partial differential equations by the finite element method*, Studentlitteratur, 1987.

[31] P. Joly, *Variational methods for time-dependent wave propagation problems, Lecture Notes in Computational Science and Engineering*, Springer, 2003.

[32] M. Krízek and P. Neittaanmaki, *Finite Element Approximation of Variational Problems and Applications*, Longman, Harlow, 1990. Zbl0708.65106, MR1066462

[33] P. B. Monk, *Finite Element methods for Maxwell's equations*, Oxford University Press, 2003.

[34] P. B. Monk and A. K. Parrott, A dispersion analysis of finite element methods for Maxwell's equations, *SIAM J.Sci.Comput.*, 15, 916-937, 1994.

[35] C. D. Munz, P. Omnes, R. Schneider, E. Sonnendrucker and U. Voss, Divergence correction techniques for Maxwell Solvers based on a hyperbolic model, *Journal of Computational Physics*, 161, 484-511, 2000.

[36] J.-C. Nédélec, Mixed finite elements in R3, *Numerische Mathematik*, 35, 315-341, 1980.

[37] K. D. Paulsen, D. R. Lynch, Elimination of vector parasites in Finite Element Maxwell solutions, *IEEE Transactions on Microwave Theory Technologies*, 39, 395 –404, 1991.

[38] Portable, Extensible Toolkit for Scientific Computation PETSc at `http://.mcs.anl.gov/petsc/`

[39] N. T. Thánh, L. Beilina, M. V. Klibanov, and M. A. Fiddy, Reconstruction of the refractive index from experimental backscattering data using a globally convergent inverse method, *SIAMJ. Sci. Comput.*, 36, B273-B293, 2014.

[40] N. T. Thánh, L. Beilina, M. V. Klibanov, M. A. Fiddy, Imaging of Buried Objects from Experimental Backscattering Time-Dependent Measurements using a Globally Convergent Inverse Algorithm, *SIAM Journal on Imaging Sciences*, 8(1), 757-786, 2015.

[41] Software package WavES at http://www.waves24.com/